Journal Pre-proofs

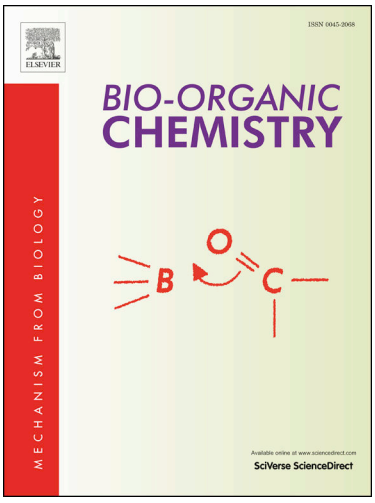

Antileishmanial effects of 4-phenyl-1-[2-(phthalimido-2-yl)ethyl]-1H-1,2,3-triazole (PT4) derivative on *Leishmania amazonensis* and *Leishmania braziliensis*: *In silico* ADMET, *in vitro* activity, docking and molecular dynamic simulations

Vanderlan Nogueira Holanda, Welson Vicente da Silva, Pedro Henrique do Nascimento, Sérgio Ruschi Bergamachi Silva, Paulo Euzébio Cabral Filho, Shalom Porto de Oliveira Assis, César Augusto da Silva, Ronaldo Nascimento de Oliveira, Regina Celia Bressan Queiroz de Figueiredo, Vera Lucia de Menezes Lima

PII: S0045-2068(20)31735-1
DOI: https://doi.org/10.1016/j.bioorg.2020.104437
Reference: YBIOO 104437

To appear in: *Bioorganic Chemistry*

Received Date: 22 July 2020
Revised Date: 30 September 2020
Accepted Date: 26 October 2020

Please cite this article as: V. Nogueira Holanda, W. Vicente da Silva, P. Henrique do Nascimento, S. Ruschi Bergamachi Silva, P. Euzébio Cabral Filho, S. Porto de Oliveira Assis, C. Augusto da Silva, R. Nascimento de Oliveira, R. Celia Bressan Queiroz de Figueiredo, V. Lucia de Menezes Lima, Antileishmanial effects of 4-phenyl-1-[2-(phthalimido-2-yl)ethyl]-1H-1,2,3-triazole (PT4) derivative on *Leishmania amazonensis* and *Leishmania braziliensis*: *In silico* ADMET, *in vitro* activity, docking and molecular dynamic simulations, *Bioorganic Chemistry* (2020), doi: https://doi.org/10.1016/j.bioorg.2020.104437

Antileishmanial effects of 4-phenyl-1-[2-(phthalimido-2-yl)ethyl]-1H-1,2,3-triazole (PT4) derivative on *Leishmania amazonensis* and *Leishmania braziliensis*: *In silico* ADMET, *in vitro* activity, docking and molecular dynamic simulations

Vanderlan Nogueira Holanda[a,b], Welson Vicente da Silva[b], Pedro Henrique do Nascimento[b], Sérgio Ruschi Bergamachi Silva[c], Paulo Euzébio Cabral Filho[d], Shalom Porto de Oliveira Assis[e], César Augusto da Silva[f]; Ronaldo Nascimento de Oliveira[g]; Regina Celia Bressan Queiroz de Figueiredo[b,1], Vera Lucia de Menezes Lima[a,*,1]

[a]Laboratório de Lipídios e Aplicação de Biomoléculas em Doenças Prevalentes e Negligenciadas. Departamento de Bioquímica, Centro de Biociências, Universidade Federal de Pernambuco, Avenida Professor Moraes Rego, 1235, 50670-901 Recife, PE, Brazil;

[b]Laboratório de Biologia Celular de Patógenos, Instituto Aggeu Magalhães, Departamento de Microbiologia, Avenida Professor Moraes Rego, 1235, 50670-901 Recife, PE, Brazil;

[c]Instituto do Cérebro, Universidade Federal do Rio Grande do Norte, Av. Nascimento de Castro, 2155 - Morro Branco, 59056-450 Natal, RN, Brazil;

[d]Departamento de Biofísica e Radiobiologia, Universidade Federal de Pernambuco, Avenida Professor Moraes Rego, 1235, 50670-901 Recife, PE, Brazil;

[e]Núcleo de Pesquisas em Ciências Ambientais e Biotecnologia, Universidade Católica de Pernambuco, Rua do Príncipe, 526, 50050-900 Recife, PE, Brazil;

[f]Colegiado de Medicina, Universidade Federal do Vale do São Francisco, Avenida José de Sá Maniçoba, s/n - Campus Universitário, 56304-205, Petrolina, PE;

[g]Laboratório de Síntese de Compostos Bioativos, Departamento de Química, Universidade Federal Rural de Pernambuco, Rua Dom Manuel de Medeiros, s/n - Dois Irmãos, 52171-900, Recife, PE, Brazil

[1]*Both authors contributed equally to this work*

*Corresponding author: *Dr. Vera Lucia de Menezes Lima. Laboratório de Lipídios e Aplicação de Biomoléculas em Doenças Prevalentes e Negligenciadas. Departamento de Bioquímica, Centro de Biociências, Universidade Federal de Pernambuco, Avenida Professor Moraes Rego, 1235, 50670-901 Recife, PE, Brazil. E-mail addres: lima.vera.ufpe@gmail.com (V. L. M. Lima)*

Abstract

Organic compounds obtained by the click chemistry reactions have demonstrated a broad spectrum of biological activities being widely applied for the development of molecules against pathogens of medical and veterinary importance. Cutaneous leishmaniasis (CL), caused by intracellular protozoa parasite of genus *Leishmania*, comprises a complex of clinical manifestations that affect the skin and mucous membranes. The available drugs for the treatment are toxic and costly, with long periods of treatment, and the emergence of resistant strains has been reported. In this study we investigated the *in vitro* effect of a phthalimide-1,2,3-triazole derivative, the 4-Phenyl-1- [2-(phthalimido-2-yl)ethyl]-1H-1,2,3-triazole (PT4) obtained by click chemistry, on mammalian cells and *L. amazonensis* and *L. braziliensis*, the causative agent of CL in Brazil. *In silico* ADMET evaluation of PT4 showed that this molecule has good pharmacokinetic properties with no violation of Lipinski's rules. The *in vitro* assay showed that PT4 was selective for both *Leishmania* species than to mammalian cells. This compound also has a low cytotoxicity to mammalian cells with CC_{50} > 500 μM. Treatment of promastigote forms with different concentrations of PT4 resulted in ultrastructural alterations, such as plasma membrane wrinkling, shortening of cell body, increased cell volume and cell rupture. The molecular dynamic simulation results showed that PT4 interacts with Lanosterol 14 α-demethylase from *Leishmania,* an essential enzyme of lipid synthesis pathway in this parasite. Our results demonstrated PT4 was effective against both species of *Leishmania*. PT4 caused a decrease of mitochondrial membrane potential and increased production of reactive oxygen species, which may lead to parasite death. Taken together, our results show pointed PT4 as promissory therapeutic agent against CL.

Keywords: Leishmaniasis, Chemotherapy, Phthalimide, 1,2,3-triazole, click chemistry.

1 Introduction

Leishmaniasis is a complex of prevalent and neglected diseases caused by protozoa of the genus *Leishmania*. The clinical manifestations of leishmaniasis range from potential fatal visceral leishmaniasis (Le Rutte *et al.*, 2019) to the most common cutaneous leishmaniasis (CL), which is characterized by the appearance of skin and mucous membrane lesions (Blum *et al.*, 2013). CL occurs in several countries of Latin America, in the Mediterranean, Middle East, and Central Asia. This disease is characterized by lesions that can lead to anatomical disfigurement of the nasal septum and ears, depending on the immune status of patient and on the *Leishmania* species (Couto *et al.*, 2014; Berbert *et al.*, 2018). Furthermore, an intense inflammatory response, characteristic of CL, may lead to tissue damage, ulcer formation, scarring, which ultimately result in social stigmatization (Maspi *et al.*, 2016).

Regardless of the clinical manifestations of Leishmaniasis, pentavalent antimonials such as sodium stibogluconate and meglumine antimoniate have been used since the early twentieth century as the first choice for the treatment of this illness (Sundar and Chakravarty, 2015). Despite of their efficacy, these drugs require long-term parenteral administration, are expensive and have adverse reactions, such as cardiotoxicity and acute renal failure (Shanehsaz and Ishkhanian, 2016). In addition, the appearance of parasite resistance has also been reported (Gervazoni *et al.*, 2018). Due to the limitations related to their pharmacokinetics and bioavailability, these drugs are not used in topical formulations. Pentamidine and amphotericin B are introduced as second-choice drugs against leishmaniasis therapy for the treatment of refractory cases. However, these drugs also have high cost and toxicity, imposing important health concerns (Oliveira *et al.*, 2011). In this regard, the search for new safe and economically viable therapeutic agents against leishmaniasis is still necessary.

Triazoles and their derivatives have attracted the attention of the scientific community due to their interesting properties as: anti-inflammatory (Tariq *et al.*, 2018), antimicrobial (Zhang, 2019), antifungal (Xie *et al.*, 2017), anticancer (Gholampour *et al.*, 2019) and antimalarial (Chu *et al.*, 2019). The heterocyclic rings of triazoles bind with high affinity to a variety of enzymes and receptors via non-covalent interactions (Shao *et al.*, 2011). These properties make 1,2,3-triazoles compounds very attractive, not only as bioactive compounds, but also as molecular blocks for organic synthesis and as functionalizes in the materials science (Dheer *et al.*, 2017; Alves *et al.*, 2018). In the last decades, with the establishment of *click chemistry* reactions, the synthesis of 1,2,3-triazoles derivatives and hybrid molecules was substantially improved. The *click chemistry* refers to a group of reactions that are low cost, fast, simple to perform, versatile, regiospecific, giving high product yield (Hein *et al.*, 2008). Furthermore, these reactions use solvents that are inoffensive and can be easily removed (Kolb *et al.*, 2001).

As the triazoles derivatives, heterocyclic molecules belonging to the phthalimide class have been also attracted attention due to their relevant biological activities such as: anticonvulsive (Kamiński *et al.*, 2011), antioxidant (Karthik *et al.*, 2015), analgesic (Alanazi *et al.*, 2015), antimicrobial (Pan *et al.*, 2016), and anti-inflammatory (Banarouei *et al.*, 2019; Batista *et al.*, 2019). Among the interesting chemical properties of phthalimides and their N-substituted derivatives, the presence of both hydrophobic aryl ring, (-CONH), which acts as a hydrogen donor, and an electron donor system (C = N) contributes for the biological activities of these molecules (Kushwaha and Kaushik, 2016).

Because the infection with *Leishmania spp*. lead to an exacerbate inflammatory response (Rodrigues *et al.*, 2015), the anti-inflammatory propriety of phthalimide and

their derivatives, allied to its putative leishmanicidal potential, could be a useful strategy to combat leishmaniasis infection.

The combination, by *click chemistry* reactions, of chemical groups having anti-inflammatory and antiparasitic action is promising for the prospection of molecules candidates for CL therapy. In this regard, previous study carried out by our group has identified a hybrid molecule phthalimide-1,2,3-triazole, 4-Phenyl-1-[2- (phthalimido-2-yl) ethyl]-1H-1,2,3-triazole (PT4) as having a potent *in vivo* anti-inflammatory activity (Assis *et al.*, 2019). Thus, in this work we selected this molecule to evaluate its leishmanicidal potential against the *Leishmania amazonensis* and *Leishmania braziliensis*, the main etiologic agents of CL in Brazil.

2 Materials and Methods

2.1 Synthesis and obtaining of 2-[2-(4-phenyl-1H-1,2,3-triazol-1-yl)ethyl]-1H-isoindole-1,3(2H)-dione (PT4). The strategy for the synthesis of 2-[2-(4-phenyl-1H-1,2,3-triazol-1-yl)ethyl]-1H-isoindole-1,3(2H)-dione (PT4) derivative was presented in Scheme 1. The compound was obtained as previously described (Sirion *et al.*, 2010). The infrared spectra were recorded with an IFS66 Bruker spectrophotometer using KBr discs. ^{1}H and ^{13}C NMR were obtained on Varian Unity Plus 400 MHz spectrometer using DMSO-d_6 as the solvent. The compounds were purified using column chromatography on Merck silica gel 60 (70-230 mesh), with a system hexane:EtOAc (1:1) ratio. The purity of fractions was monitored in TLC analysis on GF_{254} plate. The azide and 1,2,3-triazoles compounds were prepared according to the procedure described by Silva *et al.* (2012).

Scheme 1. Click reaction for PT4 synthesis

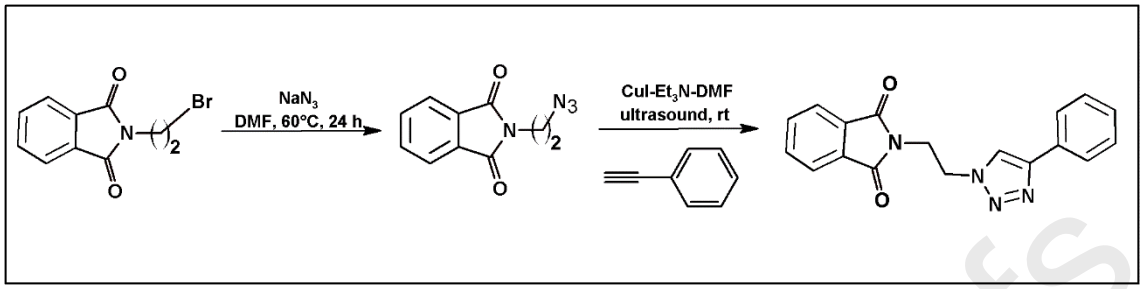

2.2 In Silico ADMET assay. Prediction of absorption, distribution, metabolism, excretion and toxicity (ADMET) parameters of PT4 and the reference drugs for leishmaniasis were performed using the online SwissADME (http://www.swissadme.ch/) platform of the Swiss Institute of Bioinformatics, PROTOX-II Server (http://tox.charite.de/protox_II / index.php? site=home) and pkCSM server (http://biosig.unimelb.edu.au/pkcsm/). The physical-chemical parameters, potential for oral bioavailability, similarities to other compounds already described were also predicted using OSIRIS Data Explorer and DataWarrior version 4.7 software (http://www.openmolecules.org/datawarrior/) and compared with the descriptors obtained for reference drugs.

2.3 Cytotoxicity Assay in Mammalian Cells. The cytotoxic potential of PT4 on macrophages (obtained from Balb/c mice peritoneal exudate (mPEC) and from J774A.1 ATCC® TIB-67 ™ linage) and fibroblast (ATCC® PCS-201-018) were assayed by MTT methodology, as established by Mosmann (1983) with slight modifications. J774 macrophages, mPEC and fibroblasts (5×10^5 cells / well) were plated in 96-well plates containing 100 μL of the RPMI (for macrophage) or DMEM (for fibroblast) medium supplemented with 10% fetal bovine serum (FBS) and maintained at 37°C for 3 h in a

5% atmosphere of CO_2. After this, the adhered cells were incubated in the absence or presence of PT4 (78.5-1,256.5 μM) in culture medium for 48h. After incubation time, the cells were washed with HBSS buffer and incubated in RPMI containing 5 mg/mL 3-(4,5-dimethylthiazol-2-yl)-2,5-diphenyltetrazolium bromide (MTT, Sigma-Aldrich, St. Louis, MO, USA) for 3h at 37 °C in the absence of light. The medium was then discarded and 100 μL of an acidified isopropanol solution (HCl 0.04 N + absolute isopropanol) was added to each well to solubilize the formazan crystals. The absorbance was read spectrophotometrically in a microplate spectrophotometer (Bio-Rad®, California, USA) at 540 nm. Each assay was performed in triplicate in three independent experiments. The cytotoxic concentration for 50% of cells (CC_{50}) was calculated by linear regression using the IBM SPSS Statistics 25.

2.4 Parasites. The promastigote forms of *Leishmania amazonensis* (LTB0016) and *Leishmania braziliensis* (LTB2903) were maintained in Schneider's medium (Sigma-Aldrich, USA) supplemented with 10% of bovine fetal serum and 100 IU penicillin and 100 IU / mL streptomycin, at 26 °C. Exponential-phase promastigotes were used in all experiments. Amastigote forms were obtained from Balb/c peritoneal macrophages infected with the stationary growth promastigote forms of the parasites.

2.5 In vitro effects of PT4 on promastigotes and amastigote of L. amazonensis and L. braziliensis. *L. amazonensis* and *L. braziliensis* promastigotes (10^6 cells / mL) were incubated in Schneider's medium in the presence or the absence of PT4 (314.1- 19.6 μM) for 48h. The culture density was determined by direct counting in a Neubauer chamber. The concentration of PT4 compound capable of inhibiting the growth of the culture by 50% (IC_{50}) was determined by linear regression analysis using the IBM SPSS

Statistics 25, after 48 hours of drug treatment. To investigate the effect of PT4 on intracellular amastigote forms, mPEC (10^6 cells/mL) were plated in 24-well plates and maintained at 37 ° C for 3h in a 5% CO_2 atmosphere. Subsequently, the adhered cells were infected with promastigotes of *L. amazonensis* and *L. braziliensis*, at 15: 1 parasite/cell ratio, at 37 °C for 14h. The non-internalized parasites were removed by washing and then the infected cells were incubated for 24 h with PT4 at concentrations corresponding to ½ IC_{50}, IC_{50} or 2x IC_{50} values, determined for promastigote forms of each species. Infected-cells cultured in drug-free medium were used as a negative control. Cells infected and treated with pentamidine (30 μM) were used as a positive control. After the incubation time, treated and untreated cells were washed with PBS, fixed with methanol and stained with Giemsa. The percentage of infected cells was determined by counting 150 randomly chosen macrophages in duplicate. The survival index was determined by multiplying the number of infected cells by the mean number of amastigotes per cell. The concentration that inhibited amastigote (IC_{50}/amastigote) growth within the macrophages was determined by regression analysis as described above. These assays were performed in duplicate in three independent experiments.

2.6. Scanning Electron Microscopy. For identify putative morphological changes induced by PT4 treatment on the parasites, scanning electron microscopy analysis were performed. For this, promastigote forms of *L. amazonensis* and *L. braziliensis* treated or not with IC_{50} or 2x IC_{50} of PT4, for 48 h were harvest by centrifugation, washed with 0.1 M phosphate buffer, pH 7.2, and then fixed for 2 h with 2.5% glutaraldehyde/4% paraformaldehyde solution, in 0.1 M phosphate buffer at pH 7.2. After the fixation, cells were allowed to adhere to coverslips previously coated with poly-L-lysine. The samples were then post-fixed with a 1% osmium tetroxide/0.8% potassium ferricyanide/5 mM

$CaCl_2$ in 0.1 M cacodylate buffer solution, at pH 7.2, for 1 hour in dark condition. After post-fixation, the samples were washed in the same buffer, dehydrated in graded ethanol series, critical-point-dried with CO_2, coated with a 20 nm-thick gold layer and observed with a JEOL T-200 scanning electron microscope.

2.7 Docking and Molecular Dynamic (MD) Simulations. The structure of PT4 was built with Avogadro software (Hanwell *et al.,* 2012) and optimized using the PM3 semi-empirical method (Stewart, 1989) implemented in Orca 4.2 (Neese, 2012). Molecular docking was performed based on the confrontation between optimized PT4 structure and the sterol 14-α-demethylase enzyme (CYP51) from *Leishmania infantum*. The docking analysis was carried out using Autodock Vina software (Trott and Olson, 2010). The crystal structure of sterol 14-α-demethylase was obtained from Protein Data Bank (PDB) under the code 3L4D (Hargrove *et al.,* 2011). Water molecules were removed, and polar hydrogens were added. The best binding poses were assessed in a 30 x 30 x 30 Å docking cube centered inside of the substrate binding cavity. The two most energetically favorable structures obtained from docking were selected as initial conformations for MD simulations. These calculations and analyses were performed for two binding poses, name $PT4_A$ and $PT4_B$, using the GROMACS 2018.4 (Abraham *et al.,* 2015; Pronk *et al.,* 2013) software package with CHARMM36 force field (Huang *et al.,* 2017). The force field topology and parameters for PT4 were obtained from CHARMM-GUI module (Kim *et al.,* 2017). The systems were solvated by 17879 SPC water molecules and counter ions Na^+ and Cl^- were added to neutralize the charge and maintain the system at a concentration of 150 mM. The protonation states of amino acid sidechains were verified by PROPKA 3.0 (Olsson *et al.,* 2011) software assuming physiological pH. Each system was submitted to the energy minimization step using

steepest descent algorithms and the equilibration period (EP) of 125 ps was made with NPT ensemble. The production runs were carried out in the NVT ensemble with a total time simulation of 100 ns for each system. The V-rescale thermostat (Bussi, Donadio and Parrinello, 2007) was used to maintain the system temperature at 310K. Other MD parameters and covalent bonds involving hydrogen atoms in the protein and water molecules were restrained by LINCS and SETTLE algorithms, respectively (Miyamoto and Kollman, 1992; Hess *et al.,* 1997). The Leap-Frog algorithm (Van Gunsteren and Berendsen, 1988) was applied to integrate the motion equation with a time step of 2.0 fs. The long-range interactions were treat using Particle-Mesh Ewald sum (PME) (Darden, York and Pedersen, 1993) with a 1.2 nm cutoff distance. The Interaction Potential Energy (IPE) and hydrogen bond evaluations were performed as we previously described (Silva *et al.,* 2017). The two systems, $PT4_A$ and $PT4_B$, present the same number of particles and the only difference is the PT4 disposition into the binding cavity.

2.8 Analysis of PT4 on mitochondrial membrane potential and reactive oxygen species production. To determine the effect of PT4 on mitochondrial membrane potential (ΔΨm), *L. amazonensis* and *L. braziliensis* promastigotes were treated with 1x or 2x IC_{50} of PT4 for 48h. After this, treated and control parasites were incubated with 10 μg/mL of rhodamine 123 (Sigma Aldrich, St. Louis, USA) for 15 min. Changes in the mitochondrial membrane polarization were measured using the Variation Index (VI) obtained by the equation **(MT − MC) / MC** where **MC** is the median fluorescence intensity of the control and **MT** the median fluorescence intensity of the treated cells. The mitochondrial reactive oxygen species production (ROS) production was assayed using the sensitive-hydroethidine-analogue mitochondrial targeted probe, MitoSOX 3,8-

phenanthridinediamine, 5-(6′-triphenylphosphoniumhexyl)-5,6 dihydro-6-phenyl (Invitrogen - Molecular Probes, USA). The cells were loaded with 2 mL of 5 μM MitoSOX reagent and incubated for 10 min at 26 °C, protected from light. After incubation, the parasites were washed three times with HBSS buffer. H_2O_2 (10 μM) was used as a positive control. For both analyses, the data collection was performed in a BD Accuri™ C6 Plus flow cytometer (BD Biosciences, USA), in a corresponding channel detection for each fluorescent probe. Twenty thousand events per sample were analyzed.

2.9 Ethical Considerations. The present research was carried out in accordance with the ethical principles adopted by Brazilian legislation 11,794 / 2008 and approved by the Instituto Aggeu Magalhães / Fundação Oswaldo Cruz Ethics Committee on Animal Research (No. 146/2019).

3 Results and Discussion

The organic synthesis of new chemotherapeutic compounds against neglected diseases, including leishmaniasis, may be hindered when the methods used are complexes, time-consuming, expensive and have low possibility of large-scale production. In a previous work we used *click chemistry* methodology to efficiently synthetize alkyl-substituted phthalimide 1H-1,2,3-triazole derivatives. Among them, the compound 2-[2-(4-phenyl-1H-1,2,3-triazol-1-yl)ethyl]-1H-isoindole-1,3(2H)-dione (PT4) derivative presenting an important anti-inflammatory activity (Assis et al., 2019) being selected for the analysis of its leishmanicidal potential on the etiological agents of CL in Brazil. This hybrid phtalimide-1,2,3 triazole compound was obtained with 93%

yield and presented the following characteristics colorless solid; mp 187-189 ºC (Lit. 157-158 ºC); Rf 0.4 (EtOAc-Hexane, 1:1); IR (KBr) ν_{max} 3126, 2952, 1774, 1716, 1464, 1432, 1396, 1231, 1078, 765, 720 cm^{-1}. The ^{1}H and ^{13}C NMR are in accordance with previously reported data (Sirion *et al.*, 2010).

In the search of new compounds against leishmaniasis the drug-likeness and absorption, distribution, metabolism and excretion (ADMET) proprieties of drug candidates should be considered (Lasing *et al.*, 2020). *In silico* ADMET is useful and low-cost method for accurate prediction of pharmacokinetic parameters and their possible interactions with cells, enzymes and biological membranes (Vijayakumar *et al.*, 2019). In this regard, *in silico* ADMET platforms were used to characterize the pharmacokinetics profile of PT4 comparing with the reference drugs glucantime (GLU), pentamidine (PEN), miltefosine (MIL) e amphotericin B (AMB) (Table 1).

Table 1. Analysis of pharmacokinetic and toxicological parameters (ADMET) of PT4 and the reference drugs used in the treatment of CL.

Parameter	**PT4**	**GLU**	**PEN**	**MIL**	**AMB**
Lipinski Rules Violation	No	Yes	No	No	Yes
Physicochemical properties					
HBA (≤10)	4	9	4	4	18
HBD (≤5)	0	7	4	0	12
LogP (≤5)	2.23	-2.90	2.72	3.83	-0.39

MW (≤500) g/mol	318.33	365.98	340.42	407.57	924.08
n-ROTB (≤10)	4	6	10	20	3
TPSA (A²)	68.09	167.55	118.20	68.40	319,61
Absorption					
BBB	Yes	No	No	No	No
GIA	High	Low	High	Low	Low
P-GP substrate	No	No	No	Yes	Yes
Skin permeability (cm/s)	-6.85	-11.34	-6.56	-3.97	-11.94
Metabolism					
CYP450 2C9 inhibitor	Yes	No	Yes	No	No
CYP450 2D6 inhibitor	No	No	Yes	No	No
CYP450 2C19 inhibitor	Yes	No	No	No	No
CYP450 3A4 inhibitor	No	No	No	No	No
CYP450 1A2 inhibitor	Yes	No	No	No	No
Excretion					
Total Clearance (log ml/min/kg)	0.117	0.895	0.814	1.112	-1.495
Renal OCT2 substrate	No	No	Yes	No	No
Toxicity					
DL_{50} (mg/Kg)	4700	3500	500	246	100

Subtitle: PEN - Pentamidine; GLU - glucantime; MIL - miltefosine; AMB - amphotericin B. Physicochemical properties: HBA - Number of hydrogen force acceptors; HBD - Number of

hydrogen donors; LogP - Octanol-water partition coefficient (lipophilicity); MW - Molecular Weight; n-ROTB - Number of rotary connections; TPSA- polar surface area. Absorption: BBB - blood-brain barrier; GIA - gastrointestinal absorption; P-gp - permeability glycoprotein; Log Kp - Skin permeation. Metabolism: CYP450 - Cytochrome P450 Enzyme; Toxicity: MUT - mutagenic; TUM - tumorigenic; IRR - annoying; LD_{50} - lethal dose up to 50%.

The Lipinski´s rule-of-five is an empirical rule of thumb which describe the physicochemical parameters to determine drug-likeness and fitter hit molecules (Lipinski *et al.*, 1997). These rules state that an orally active drug does not has more than two violation of the following parameters: 1) No more than 5 hydrogen bond donors; 2) No more than 10 hydrogen bond acceptors; 3) a molecular mass less than 500 Daltons.; 4) an octano-water partition coefficient LogP not greater than 5. According to our predictive analysis the reference drug Glucantime presented 1 violation (NH or OH>5) and Amphotericin B (AmB) had three violations (MW>500, N or O>10 and NH or OH>5). On the other hand, PT4 fulfil all the requirements of Lipinsk´s rule of five as a candidate for development of oral formulation against cutaneous leishmaniasis. Ocatanol-water partition coefficient (LogP) is a measure of hydrophobicity of a given compound. The value of LogP for PT4 was 2.23 whereas the reference drug Miltefosine was the most lipophilic molecule with LogP value of 3.83. It well known that the hydrophobicity is pivotal for drug absorption, bioavailability, hydrophobic drug receptor interactions, metabolism and cytotoxicity (Ali Khan *et al.*, 2013). PT4 presented a topological polar surface (TPSA) of 68.09 Å, which favor its permeability and oral bioavailability. It has been assumed by various predictive studies that the bioavailability and oral permeability properties decrease as the value of TPSA increases (Lagorce et al., 2017). For polarity, the optimal values of bioavailability should range between 20 and 130Å. (Daina, Michielin and Zoete, 2017). Both reference drugs

Glucantime and Amphotericin B presented higher TPSA, which impaired their passive diffusion through the BBB. The combination of the number of rotatable bound count with the TPSA reflects the flexibility of PT4. It has been demonstrated that higher TPSA/numbers of rotatable bounds can decrease the bioavailability of drugs on rat model (Lagorce *et al.*, 2017). Although PT4, Glucantime and AmB have low number of rotatable bounds, the higher values of TPSA found for the reference drugs, probably contribute for their low bioavailability profile. Additionally, in the case of CNS permeation by passive diffusion, the TPSA must be below 80 Å (Table 1).

Cytochrome P450 (CYP450) enzymes are essential for detoxification of foreign chemicals and drug metabolism in mammalian cells (Manikandan and Nagini, 2018). Our results showed PT4 as potential inhibitors of three CYP450 enzymes (CYP450 2C9, CYP450 C19, and CYP450 1A2) whereas Pentamidine was found as a potential inhibitor of CYP450 2C9 and CYP450 2D6. None of CYP450 enzymes were predicted to be inhibited by Glucantime, Miltefosine and Amphotericin B. Drugs interact with the CYP450 system in several ways. The metabolic interaction between CYP450 and drugs or xenobiotic are referred to as either inhibitors or inducers (Lynch and Price, 2007). It well documented that commercially available drugs containing triazole groups, such as Itraconazole and Posaconazole antifungals, are substrates and inhibitors CYPs (Amsden and Gubbins, 2017). To varying extents, two enzymes in the CYP3A family catalyze the metabolism of all triazole-containing drugs: CYP3A4 and CYP3A5. Interestingly, PT4 was not predicted to inhibit CYP450 3A4, suggesting that this compound, as other triazoles derivatives can be efficiently metabolized by this enzyme. Although PT4 has been predicted as inhibitors of some CYP450 enzymes, the extent to which PT4 affects these enzymes may be influenced by factors as its ability to bind the enzyme (reversibly or irreversibly), the dose and CYP450 enzyme

polymorphism. Therapeutically, further studies are needed to better understand the nature of PT4 interactions with human CYPs enzymes and other drugs.

When compared with the reference drugs for leishmaniasis, PT4 have a reduced risk of toxicity. The predicted lethal dose for murine model (LD_{50}) was 4,700 mg/kg, which were at least 1.34 and 470 higher than those found for Glucantime (3500 mg/Kg) and Amphotericin B (100 mg/Kg), the less and most toxic among the reference drugs tested. Overall, our *in silico* ADMET prediction showed that PT4 has a desirable drug-like properties and favorable safety profile.

Our *in silico* ADMET results prompted us to further investigate the *in vitro* effects of this molecule on *Leishmania amazonensis* and *Leishmania braziliensis*, as well as its cytotoxic potential on mammalian cells. For analysis of cytotoxicity of PT4 on mammalian cells, two cell types were chosen: Macrophages (peritoneal and J774) and fibroblast cells. *Leishmania spp.* is mandatory intracellular pathogens, which require macrophages for its survival and multiplication (Filardy *et al.*, 2014). Like macrophages, fibroblasts show a high degree of injury during the development of cutaneous and/or mucosal lesions in cutaneous leishmaniasis (Bogdan *et al.*, 2000). Our results showed that PT4 has an inhibitory effect on the viability of all mammalian cells tested. However, only at the higher concentration, PT4 was able to significantly decrease the percentage of viable peritoneal macrophages and fibroblast. None of PT4 concentrations tested was able to inhibit the viability of treated cells by 100% (Figure 1). The peritoneal macrophages were the most resistant to PT4 treatment, whereas J774 was the most susceptible. The CC_{50}/48h was 981.37, 521.47 and 895.17 μM for peritoneal macrophages, J774A.1 cells and fibroblasts, respectively.

Figure 1. Effect of PT4 on mammalian cells: (a) mPEC, (b) J774A macrophages and (c) fibroblasts. Values represent the mean ± standard deviation of three independent experiments in triplicate. * significant differences at $p < 0.05$. compared to untreated control.

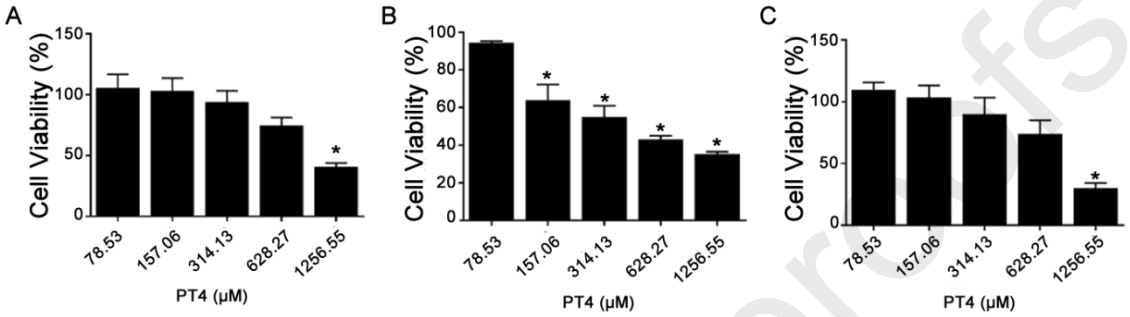

The PT4 significantly inhibited the growth of promastigote forms of both *Leishmania* species tested, in dose-dependent manner (Figure 2) for both species. *L. amazonensis* was more susceptible to PT4 treatment than *L. braziliensis* with an estimated IC_{50} of 70.46 and 181.73 µM, respectively. The biochemical/molecular differences in the susceptibility to drug between *Leishmania* species are well documented in the literature (Croft *et al.*, 2002) and can be partially explained by their distinct division rate, differential permeability, difference in plasma membrane composition and intracellular targets (Coelho *et al.*, 2016).

Figure 2. Effect of PT4 on (a) promastigote forms of *L. amazonensis* and (b) *Leishmania braziliensis*. Values represent the mean ± standard deviation of three independent experiments in triplicate. *significant differences at $p < 0.05$ compared to untreated control.

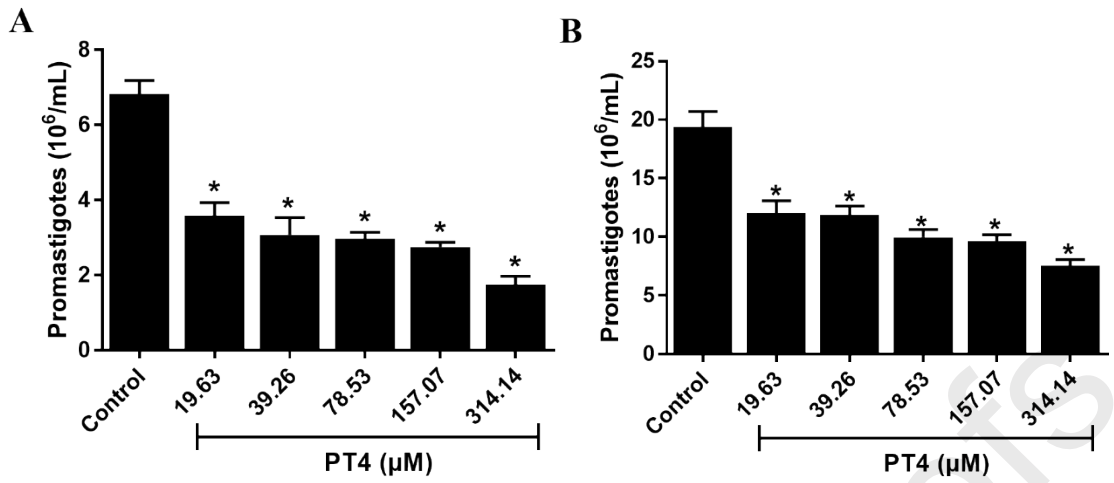

The PT4 also significantly inhibited the amastigote survival inside macrophages at all concentrations tested (Figure 3), with IC_{50} values of 125.18 and 233.18 μM for *L. amazonensis* and *L. braziliensis*, respectively. As observed for promastigote, the amastigote of *L. amazonensis* was more susceptible to the PT4 treatment. In both species, however, the amastigote was more resistant to this compound than promastigotes Although PT4 significantly inhibited the survival of amastigote inside the macrophages, only at the higher concentration (314.14 μM) this molecule was able exhibit an inhibitory activity similar to the reference drug pentamidine (PMD) at 30 μM (Figure 3). However, it is important to emphasize that pentamidine has serious collateral effects and decreasing efficacy in prolonged treatment (Sundar and Chakravarty, 2015).

Figure. 3. Effect of PT4 on intracellular amastigote forms of (a) *L. amazonensis* and (b) *L. braziliensis.* (c) Representative image of Giemsa staining showing the presence of intracellular amastigotes (black arrow) in macrophages treated or not with PT4. Values represent the mean ± standard deviation of three independent experiments in duplicate compared to untreated control, *p < 0.05.

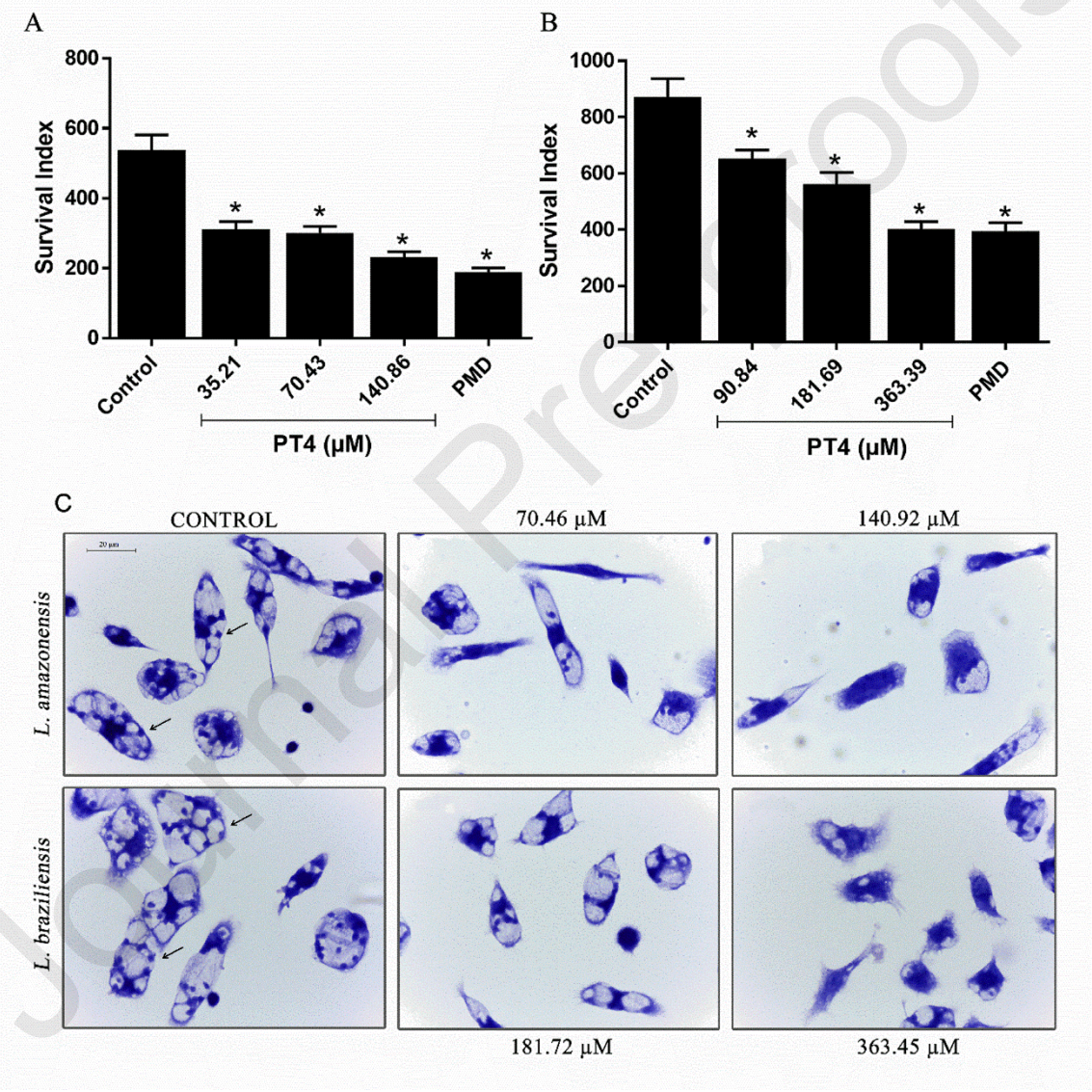

The main drawback of the chemotherapy leishmaniasis is the lack of specificity of currently available drugs used for the treatment, which often results in high toxicity to mammalian cells (Nagle *et al.*, 2014). Thus, the selectivity index (SI), i.e. the ratio of

CC_{50}, host cell cytotoxicity and IC_{50} against the parasite, is an important parameter to be taken in account in the search of new leishmanicidal agents (Papadopoulou *et al.*, 2014). Our results showed that PT4 was selective against both evolutive forms of parasite. The SI values were 13.94 and 5.40 (for promastigotes) and 7.84 and 4.21(for amastigotes) of *L. amazonensis* and *L. braziliensis,* respectively (Table 2).

Table 2. Evaluation of the leishmanicidal effect and cytotoxicity of PT4

Cell Type	**CC_{50} µM**	**$IC_{50\ (pro)}$ µM**	**$IC_{50\ (ama)}$ µM**	**Selective Index**			
				Pro		**Ama**	
				L.a	*L.b*	*L.a*	*L.b*
mPEC	982.43±5.6	-	-	13.9	5.4	7.8	4.2
J774A.1	521.47±1.2	-	-	7.4	2.8	4.1	2.2
Fib	895.17±1.2	-	-	12.7	4.9	7.1	3.8
La	-	70.46±3.5	125.05±3.2				
Lb	-	181.72±5.5	233.18±3.7	-		-	

Subtitle: mPEC - Peritoneal macrophages; CC_{50} - cytotoxic concentration in 50% of cells; IC_{50} - 50% inhibitory concentration of parasites; Pro - promastigotes; Ama - amastigotes, *L.a – Leishmania amazonensis* and *L.b – Leishmania braziliensis.*

To investigate the effects of PT4 on the ultrastructure of *L. amazonensis* and *L. braziliensis* promastigote forms, scanning electron microscopy (SEM) was performed (Figure 4). Control cells had a smooth plasma membrane, spindle-shaped body and elongated flagellum (Figures 4A-B). Drastic morphological changes could be observed

in PT4-treated cells as compared to control cells. The level of cell injuries was strongly dependent on the concentration of PT4 tested, in both *Leishmania amazonensis* (Figures 4B, 4D and 5F) and *Leishmania braziliensis* (Figures 4A, 4C and 4E). The most prominent changes observed were the increase in the cell volume (Figure 5F) with shortening and rounding of the cell body (Figure 4C). An interesting finding was the increased presence of extracellular vesicles (EVs) of different sizes budding from the cell body and flagellum in treated cells (Figures 4C and 4E). EVs are a population of lipid-enclosed spherical vesicles containing bioactive components such as soluble proteins, carbohydrates, lipids and genetic material from parental cell (Mardahl *et al.*, 2019). Commonly, EVs are classified based on their biogenesis and size into exosomes (30-150 nm in diameter), microvesicles (100-1000 nm in diameter) and apoptotic bodies (100-5000 nm in diameter). Microvesicles and exosomes have been shown to be constitutively release by several protozoan parasites, including *Leishmania* species and *T. cruzi* as a mechanism of both parasite-host and parasite-parasite communication (Mardahl *et al.*, 2019).

The increase in the EVs resembling microvesicles and exosomes in cell treated with PT4 suggests that besides their role in parasite communication EVs may also participate in the response of parasite to drugs. The large EVs, also observed budding from PT4-treated parasites, could correspond to apoptotic bodies induced by PT4 treatment (Khajah and Luqmani, 2016). PT4-treated parasites also presented incomplete division, with abnormal septation and short flagellum. These results suggest that PT4 may also have a cytostatic effect on both species of *Leishmania*.

Figure 4. Ultrastructural changes induced by PT4 on *L. braziliensis* (A, C and E) and *L. amazonensis* (B, D and F) promastigotes. Control cells (A-B), cells treated with 1x the value of IC_{50} (C-D) and 2x the value of IC_{50} (E-F).

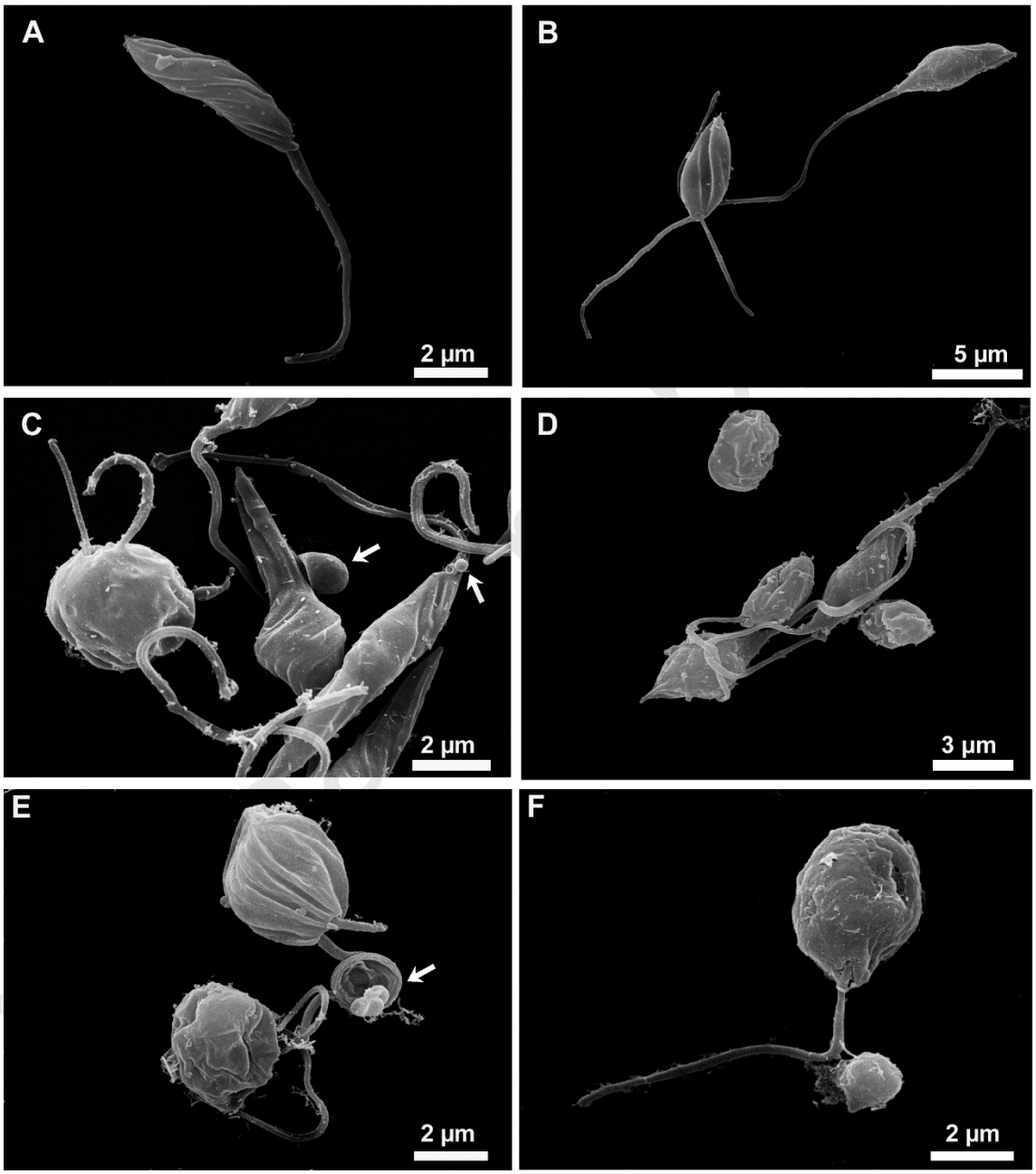

Ultrastructural changes similar to those found in our study were also observed in *Leishmania* spp. treated with triazole inhibitors of ergosterol biosynthesis (De Macedo-

Silva *et al.*, 2015). Trypanosomatids and fungi are strongly dependent on ergosterol and other 24-alkyl sterols that were not found in mammalian cells (Mccall *et al.*, 2015, Emami *et al.*, 2017). The Cytochrome P450 (CYP) is the superfamily of protoheme containing monooxygenases, found in a large number of organisms. Among P450 enzymes, sterol 14α-demethylase (CYP51), an essential enzyme in sterol biosynthesis, has been pointed as an important drug target in trypanosomatids (Lapesheva *et al.,* 2011). It has been demonstrated that commercially available anti-fungal azoles, as posaconazole and fluconazole, that inhibit the ergosterol biosynthesis in fungi are also effective against *T. cruzi* and *Leishmania* parasites (Chen *et al.*, 2010). To investigate whether PT4 could also be an inhibitor of *Leishmania* CYP51 *in silico* docking of PT4 against this enzyme was performed.

Because the crystal structure of CYP51 of *L. amazonensis* and *L. braziliensis* was not available on the protein data bank (PDB) we used the CYP51 of *L. infantum* (CYP51Li, Protein data bank entry: 3L4D) as a template for molecular docking assays and MD simulations. This protein presented 97% and 95%, of amino acid sequence similarity with two hypothetical orthologue proteins of *L. amazonensis* and *L. braziliensis*, respectively. The sequence similarity reaches 100% if we compare only the residues from the active site (Hargrove *et al.,* 2011). Previous study revealed that CYP51 is highly conserved between kinetoplastids. Chen et al., (2010) reported that a CYP51Tc from *T. cruzi* and CYP51Tb from *T. brucei* share 83% sequence identity. Furthermore, *Leishmania* CYP51 are 72–78% identical to that of *T. cruzi* and *T. brucei*. The high level of conservation of CYP51 in these parasites makes possible to extrapolate structural features that can be modeled to facilitate drug discovery and development (Chen et al., 2010).

By using CYP51L.i as receptor and the models generated from docking analysis, the MD simulations were carried out for identifying the PT4 intermolecular interaction profile. The interaction potential energy (IPE) calculations were performed to evaluate the contribution of each residue of the binding cavity and channel entrance of CYP51 receptor with the ligand. Based on non-hydrogen atoms of PT4 as reference, the RMSD analysis showed (Figure 5a) a structural stabilization around 70 ns, hence, the IPE and hydrogen bond analysis were made in the last 30 ns for both systems. The highest variation on RMSD values evidenced the motions of inhibitor inside the binding cavity and consequent settle down. The independent MD simulations taken in account two possible entering modes of PT4 molecule to an internal region of the cavity. These modes were obtained from docking analysis and indicated the first approaching of 1,2,3-triazole or phthalimide moiety to the channel of the cavity, named respectively $PT4_A$ and $PT4_B$ systems, as shown in figure 5b.

An 8 Å sphere centered on PT4 molecule was used for IPE calculation over time. This volume encompasses 62 neighboring (average) residues during the simulated time for $PT4_A$ and $PT4_B$, although most of them interact with energy very close to zero. Applying an arbitrary cutoff of IPE lower than -0.5 kcal/mol, the number of residues interacting with PT4 is 17 and 16 for $PT4_A$ and $PT4_B$, respectively. This total includes the heme group. All these most relevant residues identified by IPE calculation were presented in Table 3. They constitute the substrate channel entrance and the binding cavity described previously for the sterol 14α-demethylase receptor of *L. infantum* (Hargrove *et al.,* 2011).

Table 3. Average (standard deviation) of Interaction Potential Energy (IPE) for each residue of CYP51L.i interacting with $PT4_A$ and $PT4_B$ systems over time.

Residue	IPE (kcal/mol)	
	$PT4_A$	$PT4_B$
Tyr102	-2.84 (1.26)	-5.45 (0.96)
Phe104	-1.48 (0.59)	-2.66 (0.61)
Met105	-1.59 (0.55)	-1.97 (0.86)
Phe109	-0.61 (0.35)	-0.96 (0.56)
Tyr115	-4.16 (1.25)	-3.54 (2.14)
Leu126	-0.53 (0.37)	-0.54 (0.41)
Val212	-0.79 (0.64)	-1.19 (0.46)
Ala286	-0.66 (0.46)	-0.88 (0.54)
Phe289	-1.35 (0.60)	-0.99 (0.61)
Ala290	-2.81 (0.82)	-0.89 (0.54)
Leu355	-1.82 (0.61)	-2.42 (0.98)
Met357	-2.41 (0.96)	-3.39 (2.06)
Met359	-1.11 (0.53)	-1.10 (0.76)
Met459	-2.91 (1.58)	-1.88 (0.79)
Val460	-1.45 (0.40)	-0.86 (0.42)
Heme	-8.59 (2.13)	-14.71 (3.87)

The analysis of IPE reveals that PT4 interacts with CYP51 residues in a similar way to other antifungal azoles (Urbina *et al.,* 2000). As PT4, these nitrogenated heterocyclic compounds, contain a basic atom, which easily coordinates with heme iron (Figure 5c). The calculated IPE were -8.59 ± 2.13 kcal/mol and -14.71 ± 3.87 kcal/mol for $PT4_A$ and $PT4_B$. For $PT4_A$ orientation, the interaction occurs through triazole nitrogen with an average distance of 4.60 ± 0.39 Å and for $PT4_B$, the nitrogen of phthalimide moiety interacts with an average distance of 4.52 ± 0.38 Å. This strong interaction with the heme group plays a key role in replacing the steroid substrate becoming unfeasible for the iron reduction and consequent oxidative removal of the 14α-methyl group from the sterol core.

Among other more interacting residues presented in Table 1, Tyr102, Phe109, Tyr115 (helix B',B'/C loop), Leu126 (helix C), Ala286, Phe289, Ala290 (helix I), Leu355, Met357, Met359 (β4 strand 1-4) are constituents of substrate binding cavity (SBC) while Val212 (helix F''), Met459, Val460 (β4 hairpin) belongs to substrate channel entrance (SCE), as shown in figure 5b. Taken together, the $PT4_A$ and $PT4_B$ orientations showed similar interactions with SBC and SCE residues. Besides heme interaction, the most energetically favorable interactions take place between PT4 and a tyrosine pair belonging to the binding cavity, with -2.84 ± 1.26 kcal/mol and -4.16 ± 1.26 kcal/mol for $PT4_A$-Tyr102 and $PT4_A$-Tyr115 respectively, and -5.45 ± 0.96 kcal/mol and -3.54 ± 2.14 kcal/mol for $PT4_B$-Tyr102 and $PT4_B$-Tyr115. Together with Arg360, His420 and Arg123, both Tyr102 and Tyr115 are conserved heme-contacting residues that formed hydrogen bonds with heme propionates through their hydroxyl side chains at least 99.4% over simulated time. The conserved position of these tyrosine residues near to heme group and consequent proximity with heme-inhibitors is important for the stabilization of cavity binding via side-chain interactions through benzene ring or hydroxyl moiety. The IPE values with the other SBC residues showed their extended wrap regarding PT4 presence. In addition to helix B',B'/C loop contacts, β4 strand 1-4 and helix I structures form noncovalent interactions with benzene-like moieties of PT4 whatever entering orientation. It is noteworthy the interactions with Ala286, Phe289, Ala290 (helix I) because the high proximity with this region could be related to the better activity of heme-coordinated inhibitors. This helix acts as an anchoring point for ligand avoiding their replacement in the active site by the substrate (Lepesheva and Waterman, 2011).

Concerning the PT4 orientation inside the binding cavity, no significant differences were found on the spatial features and energetic values (Figure 5c). The total

IPE between PT4 and all surrounding residues showed similar values, -43.9 ± 3.99 kcal/mol and -49.3 ± 5.06 kcal/mol for $PT4_A$ and $PT4_B$, respectively. Due to method limitations, a bond breaking/forming cannot be assessed, hence, the Fe_{Heme}-N_{PT4} bond formation has not been described. This information could be properly evaluated by using a quantum method on further investigations. It has been already demonstrated that inactivation of the CYP51 in *Leishmania* parasites can interfere with membrane stability, increasing its fluidity, causing collapse in the membrane lipid rafts and altered morphology (Xu *et al.*, 2014).

Figure 5. MD simulation analysis and graphical representations. A) Root Mean Square Deviations (RMSD) for PT4A (green) and PT4B (orange) and one-nanosecond running averages of the deviations versus time. B) Graphical representation of the simulated system with PT4A and PT4B orientation (tubes), substrate channel entrance (red surface), substrate binding cavity (yellow surface), PT4 model inside the cavity (green tubes), heme group (blue surface) and chain A tertiary structure of sterol 14α-demethylase (CYP51) (gray cartoon). C) Superimposed view of PT4-Heme group interactions. PT4A and PT4B were differentiated through carbon coloring green and orange tubes respectively. Iron, oxygen, nitrogen and hydrogen atoms were represented by black sphere, red, blue and white tubes.

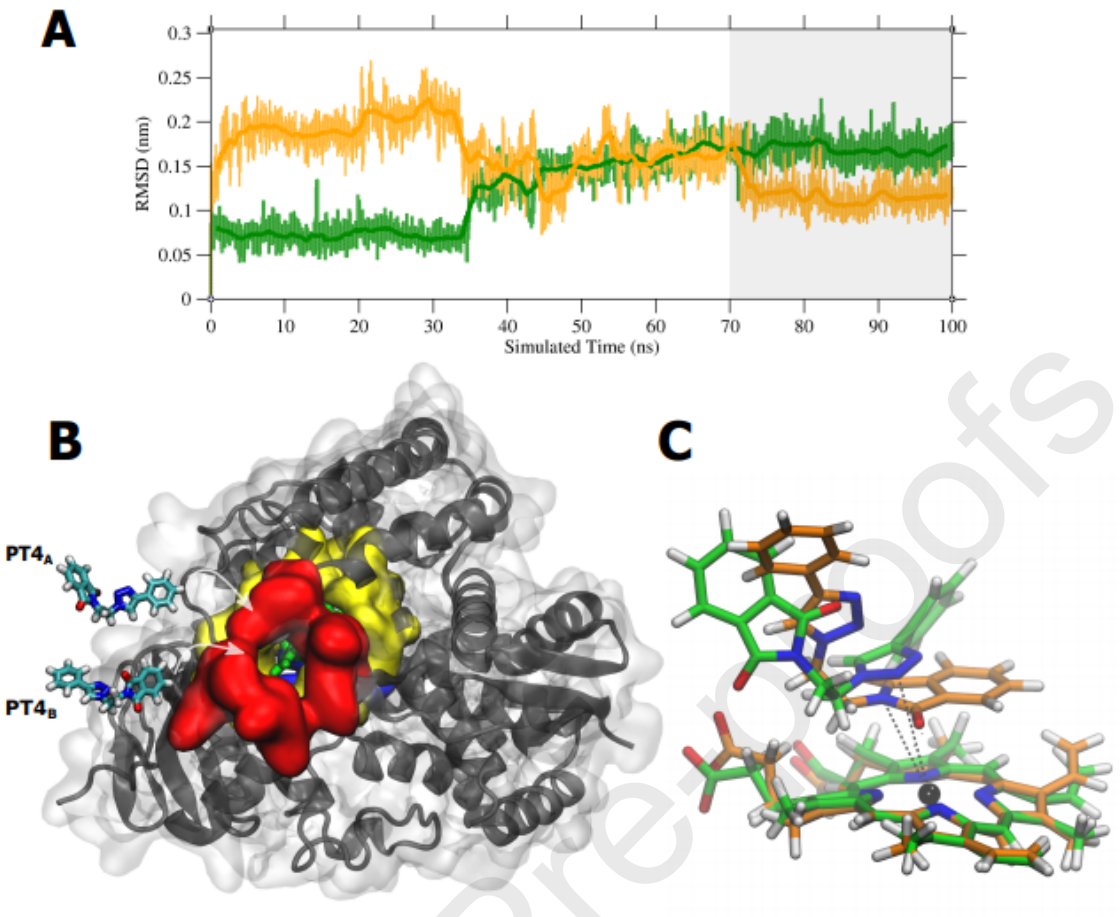

Previous work has shown that inhibition of sterol biosynthesis by triazole derivatives, alone or in combination, affects the mitochondrial function of *L. amazonensis* promastigotes by inducing a dissipation of the of mitochondrial membrane potential and increased ROS production (Macedo-Silva *et al.*, 2015). To investigate whether PT4 was able to interfere with the physiology of *L. braziliensis* and *L. amazonensis* single mitochondrion, promastigote forms were treated or not with IC_{50} and 2x IC_{50} of PT4 and submitted to staining with the fluorescent probes, Rhodamine 123 (for evaluation of mitochondrial membrane potential) and MitoSOX (for evaluation of mitochondrial ROS production). The treatment of parasites with PT4 caused a decrease in the fluorescence intensity for Rho 123 in both species and concentration tested (Table 4). Consistently, the treatment of parasites with PT4 also leading a

depolarization of mitochondrial membrane as indicated by negative values of IV (Table 4).

Table 4. Effect of PT4 on the mitochondrial membrane potential of *Leishmania amazonensis* and *Leishmania braziliensis*.

Leishmania amazonensis		
Treatment	**Rho 123 MFI**	**VI**
Control	18,635.5	-
PT4 (70.46 µM)	7,181.0	-0.61
PT4 (125.05 µM)	7,255.5	-0.61
Leishmania braziliensis		
Treatment	**Rho 123 MFI**	**VI**
Control	26,993.0	-
PT4 (181.72 µM)	5,969.0	-0.77
PT4 (363.44 µM)	7,475.5	-0.72

VI - Variation Index = MT – MC / MC, where MT is the median of fluorescence intensity in treated cells; MC is the mean of fluorescence intensity in untreated cells, MFI - median of fluorescence intensity.

Drug-induced alterations in the mitochondrial membrane potential in *Leishmania* species, have been associated with the increase in ROS, which may rupture the electron transport chain leading to mitochondrial collapse and, consequently, to cell death (Menna-Barreto and De Castro, 2014). Thus, we investigated if the loss of mitochondrial membrane potential, induced by PT treatment, was followed by a shift of mitochondrial ROS production in promastigote forms of *L. amazonensis* and *L. braziliensis* (Figure 6).

Figure 6. Representative flow cytometric histograms of the effects of PT4 on ROS production in *L. amazonensis* (A) and *L. braziliensis* (B) promastigote forms, labelled with MitoSOX. Cells without treatment and treated with H_2O_2 were considered as negative and positive control respectively.

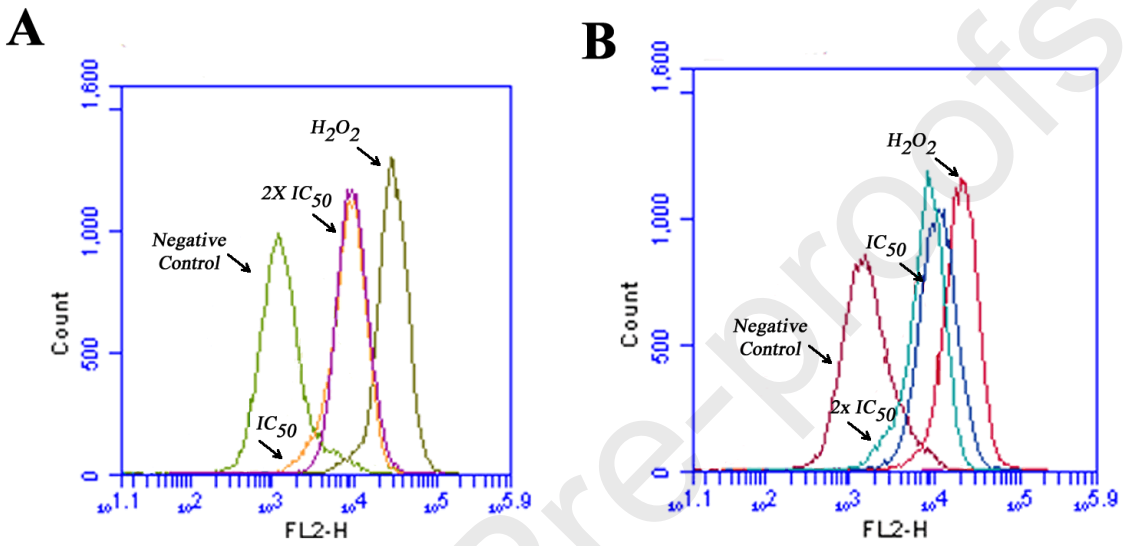

Our results showed an increased in the intensity of MitoSOX fluorescent signal in both *Leishmania* species treated with PT4, as observed by the displacement of fluorescence intensity curves to right in treated parasites, compared to control without treatment (negative control). Our results suggested that PT4 induces mitochondrial dysfunction with marked reduction of ΔΨm and increased ROS production. The increased ROS production in the single mitochondrion of *Leishmania* species, associated with mitochondrial membrane potential dissipation can lead the parasites to death (Meinel *et al.*, 2020). Previous studies showed that molecules containing 1,2,3-triazole and phthalimide groups have a high potential to interfere with mitochondrial physiology by altering membrane potential and increasing ROS (Aliança *et al.*, 2017).

4 Conclusions

Our results showed that the compound 2-[2-(4-phenyl-1H-1,2,3-triazol-1-yl)ethyl]-1H-isoindole-1,3(2H)-dione (PT4), synthetized by click chemistry has good predicted pharmacokinetic properties which can be useful for development of oral formulation for the treatment of leishmaniasis. We also demonstrated that this compound was highly selective for the parasites inhibiting the growth and survival of promastigote and amastigote forms of *L. amazonensis* and *L. braziliensis*. The ultrastructural changes induced by PT4 and PI labelling corroborate the deleterious effects of this compound on the parasite membrane in both *Leishmania* species. Our molecular docking and molecular dynamic analysis pointed PT4 as a putative inhibitor of parasite sterol 14 α-demethylase, mainly by interacting with heme groups of this enzyme. The PT4 also caused dissipation of mitochondrial potential and increased production of mitochondrial ROS in *L. amazonensis* and *L. braziliensis.* Altogether, our results support further investigation PT4 as a promising agent for the treatment of CL.

5 Acknowledgments

This work was supported by the Fundação de Amparo à Ciência e Tecnologia do Estado de Pernambuco (FACEPE), Conselho Nacional de Desenvolvimento Científico e Tecnológico (CNPq), Coordenação de Aperfeiçoamento de Pessoal de Nível Superior (CAPES), Instituto Aggeu Magalhães / FIOCRUZ-PE. We would like to thank the Prof. Dr. Norberto Monteiro (Federal University of Ceará - Brazil) for providing computational resources used for MD simulations and analysis. **Vanderlan Holanda**: Conceptualization, Methodology, Investigation, formal analysis, writing-original draft; **Welson Silva** and **Pedro Nascimento**: Investigation, formal analysis; **Sérgio Ruschi,**

Shalom Assis, Ronaldo Oliveira and **César da Silva**: Resources and Investigation; **Regina Figueiredo**: Conceptualization, Methodology, Writing-Review, Visualization. Project administration, funding acquisition, **Vera Lima**: Conceptualization, Methodology, Writing-Review, Visualization.

6 Funding

This work was supported by the Fundação de Amparo à Ciência e Tecnologia do Estado de Pernambuco (FACEPE), Conselho Nacional de Desenvolvimento Científico e Tecnológico (PQ-400749/219-0), Coordenação de Aperfeiçoamento de Pessoal de Nível Superior (CAPES), Instituto Aggeu Magalhães and Inova-Fiocruz Program (VPPCB-007-FIO-18-2-85).

7 References

Abraham, M. J. et al. GROMACS: High performance molecular simulations through multi-level parallelism from laptops to supercomputers. **SoftwareX**, v. 1, p. 19-25, 2015. doi: https://doi.org/10.1016/j.softx.2015.06.001

Alanazi, A. M. et al. Structure-based design of phthalimide derivatives as potential cyclooxygenase-2 (COX-2) inhibitors: Anti-inflammatory and analgesic activities. **European Journal of Medicinal Chemistry,** v. 92, p. 115-123, 2015/03/06/ 2015. ISSN 0223-5234. doi: https://doi.org/10.1016/j.ejmech.2014.12.039

Aliança, A. S. D. S. et al. In vitro evaluation of cytotoxicity and leishmanicidal activity of phthalimido-thiazole derivatives. **European Journal of Pharmaceutical Sciences,** v. 105, p. 1-10, 2017/07/15/ 2017. ISSN 0928-0987. doi: https://doi.org/10.1016/j.ejps.2017.05.005

Alves, D. et al. Copper Catalysis and Organocatalysis Showing the Way: Synthesis of Selenium-Containing Highly Functionalized 1,2,3-Triazoles. **The Chemical Record,** v. 18, n. 5, p. 527-542, 2018/05/01 2018. ISSN 1527-8999. doi: https://doi.org/10.1002/tcr.201700058

Amsden, J. R.; Gubbins, P. O. Pharmacogenomics of triazole antifungal agents: implications for safety, tolerability and efficacy. **Expert Opinion on Drug Metabolism & Toxicology,** v. 13, n. 11, p. 1135-1146. doi: https://doi.org/10.1080/17425255.2017.1391213

Assis, S. P. O. et al. Design and synthesis of triazole-phthalimide hybrids with anti-inflammatory activity. **Chemical and Pharmaceutical Bulletin,** v. 67, n. 2, p. 96-105, 2019. ISSN 0009-2363. doi: 10.1248/cpb.c18-00607

Banarouei, N. et al. N-arylmethylideneaminophthalimide: Design, Synthesis and Evaluation as Analgesic and Anti-inflammatory Agents. **Mini reviews in medicinal chemistry,** v. 19, n. 8, p. 679-687, 2019. doi: https://doi.org/10.2174/1389557518666180424101009

Batista, C. R. A. et al. The phthalimide analogues N-3-hydroxypropylphthalimide and N-carboxymethyl-3-nitrophthalimide exhibit activity in experimental models of inflammatory and neuropathic pain. **Pharmacological Reports,** v. 71, n. 6, p. 1177-1183, 2019/12/01/ 2019. doi: https://doi.org/10.1016/j.pharep.2019.08.001

Berbert, T. R. N. et al. Pentavalent Antimonials Combined with Other Therapeutic Alternatives for the Treatment of Cutaneous and Mucocutaneous Leishmaniasis: A Systematic Review. **Dermatology Research and Practice,** v. 2018, p. 9014726, 2018/12/24 2018. doi: https://doi.org/10.1155/2018/9014726

Blum, J. et al. LeishMan Recommendations for Treatment of Cutaneous and Mucosal Leishmaniasis in Travelers, 2014. **Journal of Travel Medicine,** v. 21, n. 2, p. 116-129, 2013. doi: https://doi.org/10.1111/jtm.12089

Bogdan, C. et al. Fibroblasts as Host Cells in Latent Leishmaniosis. **Journal of Experimental Medicine,** v. 191, n. 12, p. 2121-2130, 2000. doi: https://doi.org/10.1084/jem.191.12.2121

Bussi, G.; Donadio, D.; Parrinello, M. Canonical sampling through velocity rescaling. **The Journal of Chemical Physics**, v. 126, n. 1, p. 014101, 2007. doi: https://doi.org/10.1063/1.2408420

Chu, X.-M. et al. Triazole derivatives and their antiplasmodial and antimalarial activities. **European Journal of Medicinal Chemistry,** v. 166, p. 206-223, 2019/03/15/ 2019. doi: https://doi.org/10.1016/j.ejmech.2019.01.047

Coelho, A. C. et al. In vitro and in vivo miltefosine susceptibility of a Leishmania amazonensis isolate from a patient with diffuse cutaneous leishmaniasis: follow-up. **PLoS neglected tropical diseases,** v. 10, n. 7, p. e0004720, 2016. doi: https://doi.org/10.1371/journal.pntd.0004720

Couto, D. V. et al. American tegumentary leishmaniasis - a case of therapeutic challenge. **Anais Brasileiros de Dermatologia,** v. 89, p. 974-976, 2014. doi: https://doi.org/10.1590/abd1806-4841.20143073

Croft, S. L.; Yardley, V.; Kendrick, H. Drug sensitivity of Leishmania species: some unresolved problems. **Transactions of the Royal Society of Tropical Medicine and Hygiene,** v. 96, p. S127-S129, 2002/04/01/ 2002. ISSN 0035-9203. doi: https://doi.org/10.1016/S0035-9203(02)90063-5

Darden, T.; York, D.; Pedersen, L. Particle mesh Ewald: An N· log (N) method for Ewald sums in large systems. **The Journal of Chemical Physics**, v. 98, n. 12, p. 10089-10092, 1993. doi: https://doi.org/10.1063/1.464397

Dheer, D.; Singh, V.; Shankar, R. Medicinal attributes of 1,2,3-triazoles: Current developments. **Bioorganic Chemistry,** v. 71, p. 30-54, 2017/04/01/ 2017. doi: https://doi.org/10.1016/j.bioorg.2017.01.010

Emami, S.; Tavangar, P.; Keighobadi, M. An overview of azoles targeting sterol 14α-demethylase for antileishmanial therapy. **European Journal of Medicinal Chemistry,** v. 135, p. 241-259, 2017/07/28/ 2017. doi: https://doi.org/10.1016/j.ejmech.2017.04.044

Filardy, A. A. et al. Infection with Leishmania major induces a cellular stress response in macrophages. **PLoS One,** v. 9, n. 1, p. e85715, 2014. doi: https://doi.org/10.1371/journal.pone.0085715

Gervazoni, L. F.; Gonçalves-Ozório, G.; Almeida-Amaral, E. E. 2'-Hydroxyflavanone activity in vitro and in vivo against wild-type and antimony-resistant Leishmania amazonensis. **PLoS neglected tropical diseases,** v. 12, n. 12, p. e0006930, 2018. doi: https://doi.org/10.1371/journal.pntd.0006930

Gholampour, M. et al. Click chemistry-assisted synthesis of novel aminonaphthoquinone-1,2,3-triazole hybrids and investigation of their cytotoxicity and cancer cell cycle alterations. **Bioorganic Chemistry,** v. 88, p. 102967, 2019. doi: https://doi.org/10.1016/j.bioorg.2019.102967

Hanwell, M. D. et al. Avogadro: an advanced semantic chemical editor, visualization, and analysis platform. **Journal of Cheminformatics**, v. 4, n. 1, p. 17, 2012.

Hargrove, T. Y. et al. Substrate preferences and catalytic parameters determined by structural characteristics of sterol 14α-demethylase (CYP51) from Leishmania infantum. **Journal of Biological Chemistry**, v. 286, n. 30, p. 26838-26848, 2011. doi: 10.1074/jbc.M111.237099

Hein, C. D.; Liu, X. M.; Wang, D. Click Chemistry, A Powerful Tool for Pharmaceutical Sciences. **Pharmaceutical Research,** v. 25, n. 10, p. 2216-2230, 2008. doi: https://doi.org/10.1007/s11095-008-9616-1

Hess, B. et al. LINCS: a linear constraint solver for molecular simulations. **Journal of Computational Chemistry**, v. 18, n. 12, p. 1463-1472, 1997. doi: https://doi.org/10.1002/(SICI)1096-987X(199709)18:12<1463::AID-JCC4>3.0.CO;2-H

Huang, J. et al. CHARMM36m: an improved force field for folded and intrinsically disordered proteins. **Nature Methods**, v. 14, n. 1, p. 71-73, 2017. doi: https://doi.org/10.1038/nmeth.4067

Kamiński, K. et al. Synthesis and anticonvulsant properties of new acetamide derivatives of phthalimide, and its saturated cyclohexane and norbornene analogs. **European Journal of Medicinal Chemistry,** v. 46, n. 9, p. 4634-4641, 2011. doi: https://doi.org/10.1016/j.ejmech.2011.07.043

Karthik, C. S.; Mallesha, L.; Mallu, P. Investigation of antioxidant properties of phthalimide derivatives. **Canadian Chemical Transactions,** v. 3, p. 199-206, 2015. doi: :10.13179/canchemtrans.2015.03.02.0194

Khan, A. A. et al. Advanced drug delivery to the lymphatic system: lipid-based nanoformulations. **International Journal of Nanomedicine,** v. 8, p. 2733-2744, 2013. ISSN 1178-2013 1176-9114. doi: 10.2147/IJN.S41521

Khajah, M. A.; Luqmani, Y. A. Involvement of Membrane Blebbing in Immunological Disorders and Cancer. **Medical Principles and Practice,** v. 25, p. 18-27, 2016. doi: https://doi.org/10.1159/000441848

Kim, S. et al. CHARMM-GUI ligand reader and modeler for CHARMM force field generation of small molecules. **Journal of Computational Chemistry**, v. 38, n. 21, p. 1879-1886, 2017. doi: https://doi.org/10.1002/jcc.24829

Kolb, H. C.; Finn, M. G.; Sharpless, K. B. Click Chemistry: Diverse Chemical Function from a Few Good Reactions. **Angewandte Chemie International Edition,** v. 40, n. 11, p. 2004-2021, 2001. doi: https://doi.org/10.1002/1521-3773(20010601)40:11<2004::AID-ANIE2004>3.0.CO;2-5

Kushwaha, N.; Kaushik, D. Recent advances and future prospects of phthalimide derivatives. **Journal of Applied Pharmaceutical Science,** v. 6, n. 03, p. 159-171, 2016. doi:10.7324/JAPS.2016.60330

Lagorce, D. et al. Computational analysis of calculated physicochemical and ADMET properties of protein-protein interaction inhibitors. **Scientific Reports,** v. 7, n. 1, p. 46277, 2017. doi: https://doi.org/10.1038/srep46277

Lasing, T. et al. Synthesis and antileishmanial activity of fluorinated rhodacyanine analogues: The 'fluorine-walk' analysis. **Bioorganic & Medicinal Chemistry,** v. 28, n. 1, p. 115187, 2020. doi: https://doi.org/10.1016/j.bmc.2019.115187

Lepesheva, G. I.; Villalta, F.; Waterman, M. R. Targeting Trypanosoma cruzi sterol 14α-demethylase (CYP51). In: **Advances in parasitology**. Academic Press, 2011. p. 65-87. doi: https://doi.org/10.1016/B978-0-12-385863-4.00004-6

Lepesheva, G.; R Waterman, M. Sterol 14alpha-demethylase (CYP51) as a therapeutic target for human trypanosomiasis and leishmaniasis. **Current Topics in Medicinal Chemistry**, v. 11, n. 16, p. 2060-2071, 2011. Doi: https://doi.org/10.2174/156802611796575902

Le Rutte, E. A.; Zijlstra, E. E.; Vlas, S. J. Post-Kala-Azar Dermal Leishmaniasis as a Reservoir for Visceral Leishmaniasis Transmission. **Trends in Parasitology,** v. 35, n. 8, p. 590-592, 2019. doi: https://doi.org/10.1016/j.pt.2019.06.007

Lipinski, C. A. et al. Experimental and computational approaches to estimate solubility and permeability in drug discovery and development settings. **Advanced Drug Delivery Reviews,** v. 23, n. 1, p. 3-25, 1997. doi: https://doi.org/10.1016/S0169-409X(96)00423-1

López-Camacho, E. et al. Solving molecular flexible docking problems with metaheuristics: A comparative study. **Applied Soft Computing,** v. 28, p. 379-393, 2015. doi: https://doi.org/10.1016/j.asoc.2014.10.049

Lynch, T.; Price, A. L. The effect of cytochrome P450 metabolism on drug response, interactions, and adverse effects. **American family physician,** v. 76, n. 3, p. 391-396, 2007. ISSN 0002-838X.

Macedo-Silva, S. T. et al. Potent In Vitro Antiproliferative Synergism of Combinations of Ergosterol Biosynthesis Inhibitors against Leishmania amazonensis. **Antimicrobial Agents and Chemotherapy,** v. 59, n. 10, p. 6402, 2015. doi: 10.1128/AAC.01150-15

Manikandan, P.; Nagini, S. Cytochrome P450 structure, function and clinical significance: a review. **Current drug targets,** v. 19, n. 1, p. 38-54, 2018. ISSN 1389-4501. doi: https://doi.org/10.2174/1389450118666170125144557

Mardahl, M.; Borup, A.; Nejsum, P. A new level of complexity in parasite-host interaction: The role of extracellular vesicles. In: ROLLINSON, D. e STOTHARD, J. R. (Ed.). **Advances in Parasitology**: Academic Press, v.104, p.39-112, 2019. doi: https://doi.org/10.1016/bs.apar.2019.02.003

Maspi, N.; Abdoli, A.; Ghaffarifar, F. Pro-and anti-inflammatory cytokines in cutaneous leishmaniasis: a review. **Pathogens and global health,** v. 110, n. 6, p. 247-260, 2016. doi: ttps://doi.org/10.1080/20477724.2016.1232042

McCall, L.-I. et al. Targeting Ergosterol Biosynthesis in Leishmania donovani: Essentiality of Sterol 14alpha-demethylase. **PLOS Neglected Tropical Diseases,** v. 9, n. 3, p. e0003588, 2015. doi: https://doi.org/10.1371/journal.pntd.0003588

Meinel, R. S. et al. Novel functionalized 1,2,3-triazole derivatives exhibit antileishmanial activity, increase in total and mitochondrial-ROS and depolarization of mitochondrial membrane potential of Leishmania amazonensis. **Chemico-Biological Interactions,** v. 315, p. 108850, 2020. doi: https://doi.org/10.1016/j.cbi.2019.108850

Menna-Barreto, R. F. S.; Castro, S. L. The Double-Edged Sword in Pathogenic Trypanosomatids: The Pivotal Role of Mitochondria in Oxidative Stress and Bioenergetics. **BioMed Research International,** v. 2014, p. 614014, 2014. doi: https://doi.org/10.1155/2014/614014

Miyamoto, S.; Kollman, P. A. Settle: An analytical version of the SHAKE and RATTLE algorithm for rigid water models. **Journal of Computational Chemistry**, v. 13, n. 8, p. 952-962, 1992. doi: https://doi.org/10.1002/jcc.540130805

Nagle, A. S. et al. Recent Developments in Drug Discovery for Leishmaniasis and Human African Trypanosomiasis. **Chemical Reviews,** v. 114, n. 22, p. 11305-11347, 2014/11/26 2014. ISSN 0009-2665. doi: https://doi.org/10.1021/cr500365f

Neese, F. The ORCA program system. **Wiley Interdisciplinary Reviews: Computational Molecular Science**, v. 2, n. 1, p. 73-78, 2012. doi: https://doi.org/10.1002/wcms.81

Oliveira, L. F. et al. Systematic review of the adverse effects of cutaneous leishmaniasis treatment in the New World. **Acta Tropica,** v. 118, n. 2, p. 87-96, 2011. doi: https://doi.org/10.1016/j.actatropica.2011.02.007

Olsson, M. H. M. et al. PROPKA3: consistent treatment of internal and surface residues in empirical p K a predictions. **Journal of Chemical Theory and Computation**, v. 7, n. 2, p. 525-537, 2011. doi: https://doi.org/10.1021/ct100578z

Pan, L. et al. Synthesis of N-substituted phthalimides and their antifungal activity against Alternaria solani and Botrytis cinerea. **Microbial Pathogenesis,** v. 95, p. 186-192, 2016. doi: https://doi.org/10.1016/j.micpath.2016.04.012

Papadopoulou, M. V. et al. Novel nitro(triazole/imidazole)-based heteroarylamides/sulfonamides as potential antitrypanosomal agents. **European Journal of Medicinal Chemistry,** v. 87, p. 79-88, 2014. doi: https://doi.org/10.1016/j.ejmech.2014.09.045

Pronk, S. et al. GROMACS 4.5: a high-throughput and highly parallel open source molecular simulation toolkit. **Bioinformatics**, v. 29, n. 7, p. 845-854, 2013. doi: https://doi.org/10.1093/bioinformatics/btt055

Rodrigues, I. A. et al. Natural Products: Insights into Leishmaniasis Inflammatory Response. **Mediators of Inflammation,** v. 2015, p. 835910, 2015. doi: https://doi.org/10.1155/2015/835910

Silva, S. B. et al. The role of local residue environmental changes in thermostable mutants of the GH11 xylanase from Bacillus subtilis. **International Journal of**

Biological Macromolecules, v. 97, p. 574-584, 2017. doi: https://doi.org/10.1016/j.ijbiomac.2017.01.054

Shanehsaz, S. M.; Ishkhanian, S. Electrocardiographic and biochemical adverse effects of meglumine antimoniate (MA) during treatment of Syrian cutaneous leishmaniasis patients. **Journal of Pakistan Association of Dermatology,** v. 23, n. 4, p. 412-417, 2016.

Shao, C. et al. Acid–Base Jointly Promoted Copper(I)-Catalyzed Azide–Alkyne Cycloaddition. **The Journal of Organic Chemistry,** v. 76, n. 16, p. 6832-6836, 2011. doi: https://doi.org/10.1021/jo200869a

Silva, M. T. D. et al. Synthesis of N-substituted phthalimidoalkyl 1H-1,2,3-triazoles: a molecular diversity combining click chemistry and ultrasound irradiation. **Journal of the Brazilian Chemical Society,** v. 23, p. 1839-1843, 2012. doi: https://doi.org/10.1590/S0103-50532012005000053

Sirion, U. et al. Azide/alkyne resins for quick preparation of 1, 4-disubstituted 1, 2, 3-triazoles. **Bulletin of the Korean Chemical Society,** v. 31, n. 7, p. 1843, 2010. doi: 10.5012/bkcs.2010.31.7.1843

Stewart, J. J. P. Optimization of parameters for semiempirical methods I. Method. **Journal of Computational Chemistry**, 10: 209-220. 1989. doi:10.1002/jcc.540100208

Sundar, S.; Chakravarty, J. An update on pharmacotherapy for leishmaniasis. **Expert Opinion on Pharmacotherapy,** v. 16, n. 2, p. 237-252, 2015. doi: https://doi.org/10.1517/14656566.2015.973850

Tariq, S. et al. 1,2,4-Triazole-based benzothiazole/benzoxazole derivatives: Design, synthesis, p38α MAP kinase inhibition, anti-inflammatory activity and molecular docking studies. **Bioorganic Chemistry,** v. 81, p. 630-641, 2018/12/01/ 2018. doi: https://doi.org/10.1016/j.bioorg.2018.09.015

Trott, O.; Olson, A. J. AutoDock Vina: improving the speed and accuracy of docking with a new scoring function, efficient optimization, and multithreading. **Journal of Computational Chemistry**, v. 31, n. 2, p. 455-461, 2010. doi: https://doi.org/10.1002/jcc.21334

Urbina, J. A. et al. In vitro antiproliferative effects and mechanism of action of the new triazole derivative UR-9825 against the protozoan parasite Trypanosoma (Schizotrypanum) cruzi. **Antimicrobial Agents and Chemotherapy**, v. 44, n. 9, p. 2498-2502, 2000. doi: 10.1128/AAC.44.9.2498-2502.2000

Van Gunsteren, W. F.; Berendsen, H. J. C. A leap-frog algorithm for stochastic dynamics. **Molecular Simulation**, v. 1, n. 3, p. 173-185, 1988. doi: https://doi.org/10.1080/08927028808080941

Vijayakumar, S. et al. A pharmacoinformatic approach on Cannabinoid receptor 2 (CB2) and different small molecules: Homology modelling, molecular docking, MD

simulations, drug designing and ADME analysis. **Computational Biology and Chemistry,** v. 78, p. 95-107, 2019. doi: https://doi.org/10.1016/j.compbiolchem.2018.11.013

Xie, F. et al. Design, synthesis, and in vitro evaluation of novel antifungal triazoles. **Bioorganic & Medicinal Chemistry Letters,** v. 27, n. 10, p. 2171-2173, 2017. doi: https://doi.org/10.1016/j.bmcl.2017.03.062

Xu, W. et al. Sterol Biosynthesis Is Required for Heat Resistance but Not Extracellular Survival in Leishmania. **PLOS Pathogens,** v. 10, n. 10, p. e1004427, 2014. doi: https://doi.org/10.1371/journal.ppat.1004427

Zhang, B. Comprehensive review on the anti-bacterial activity of 1,2,3-triazole hybrids. **European Journal of Medicinal Chemistry,** v. 168, p. 357-372, 2019. doi: https://doi.org/10.1016/j.ejmech.2019.02.055

Highlights

- The leishmanicidal activity of a triazole-phthalimide derivative (PT4) was evaluated;
- PT4 decrease the growth and survival of promastigote and amastigotes;
- PT4 showed inhibitory potential over the CYP51 enzyme of *Leishmania* spp;
- PT4 induced an increase in ROS and depolarization of the mitochondrial membrane;
- Our results pointed PT4 as a promissory agent against Cutaneous Leishmaniasis.